International Journal of Heat and Technology
Vol. 43, No. 2, April, 2025, pp. 570-582
Journal homepage: http://iieta.org/journals/ijht

BIM-Enabled Optimization of Thermodynamic Performance in Green Buildings

Yinan Wu*, Bin Dai

College of Urban and Rural Construction, Hebei Agricultural University, Baoding 071000, China

Corresponding Author Email: wuyinan2005@126.com

https://doi.org/10.18280/ijht.430219

Received: 8 October 2024
Revised: 30 January 2025
Accepted: 17 February 2025
Available online: 30 April 2025

Keywords:
green building, BIM, thermodynamic performance, multi-objective optimization, indoor thermal comfort compliance rate verification

ABSTRACT

Against the backdrop of global climate change and the "dual carbon" targets, the optimization of thermodynamic performance in green buildings has emerged as a critical strategy for enhancing energy efficiency and indoor environmental quality. Building Information Modeling (BIM) provides a comprehensive platform for life-cycle data integration, supporting performance analysis in green building design. However, current practices face challenges in multi-objective collaborative optimization and in the underutilization of the latent value embedded in BIM data. Existing studies have predominantly focused on single-objective optimizations or have relied on simplified thermodynamic models, often neglecting the integrated consideration of carbon emissions, thermal comfort, and the advanced application of granular BIM data. Furthermore, research on indoor thermal comfort has lacked dynamic coupling validation of green envelope performance and has failed to establish a closed-loop "optimization–verification" mechanism. To address these limitations, a BIM-based multi-objective optimization framework was proposed for the thermodynamic performance of green buildings. This framework integrates objectives, including energy consumption, carbon emission intensity, hygrothermal performance, and indoor thermal comfort potential. A synergistic optimization of envelope parameters and spatial configurations was achieved through the coupling of intelligent algorithms with BIM-based models. Based on the optimized scheme, the thermal comfort compliance rate was verified by incorporating green envelope performance, and the Predicted Mean Vote (PMV) index was calculated to evaluate compliance across various scenarios, enabling reverse calibration of the model. A data-driven technical chain encompassing multi-objective optimization and performance verification was established in this study, offering a quantifiable design foundation that balances energy efficiency and thermal comfort, thereby extending the application potential of BIM in performance-oriented building design.

1. INTRODUCTION

Against the backdrop of global climate change and the "dual carbon" targets, green buildings have been positioned as a core mechanism for achieving energy conservation and emissions reduction in the built environment [1, 2]. The optimization of thermodynamic performance in green buildings has been recognized as a critical pathway for enhancing energy efficiency and improving indoor environmental quality [3]. The thermodynamic performance involves not only the coupling between the thermal parameters of envelope structures and building energy consumption but also requires the simultaneous consideration of indoor thermal comfort, carbon emissions control, and other multi-dimensional performance demands [4-6]. BIM, with its capability for life-cycle data integration, enables precise digital representation of architectural geometry, material properties, and climatic parameters [7-9], laying a digital foundation for the thermodynamic performance analysis of green buildings. Nevertheless, several critical challenges persist in the performance optimization of current green building design practices, including the inherent difficulty of coordinating multiple performance objectives and the insufficient extraction of embedded value within datasets [10]. A pressing issue in this field lies in how BIM-driven data can be leveraged during the early design phase to systematically optimize multiple objectives—namely, energy consumption, carbon emissions, and thermal comfort—while enabling the performance parameters of the building envelope to be validated against indoor thermal environment quality.

Advancing research on BIM-based thermodynamic performance optimization in green buildings holds significant theoretical and practical implications for promoting the green transformation of the construction industry. From a theoretical perspective, by establishing a mapping relationship between BIM data and thermodynamic performance objectives, the methodological framework for performance-oriented green building design can be expanded, providing a new paradigm for interdisciplinary integration. From a practical perspective, the precise modeling of envelope structures and spatial configurations enabled by BIM facilitates early identification of thermodynamic performance bottlenecks. By applying multi-objective optimization algorithms, a design solution that balances energy efficiency and thermal comfort can be generated. Furthermore, the feasibility of the solution can be ensured through the verification of the indoor thermal comfort compliance rate. This integrated process reduces energy consumption costs and retrofit risks during the operational phase, accelerating the transformation of green buildings from a conceptual emphasis on energy conservation to the realization of performance-based outcomes.

In existing research, several studies have concentrated on BIM-based building energy simulations and single-objective optimization [11-14]. However, such approaches have frequently failed to consider the coordinated optimization of objectives such as carbon emissions and thermal comfort, resulting in design contradictions characterized by either "energy-efficient but uncomfortable" or "comfortable but high-carbon" outcomes. Although attempts have been made to introduce multi-objective optimization algorithms, these efforts have largely relied on simplified thermodynamic models and have not sufficiently leveraged the high-resolution data embedded in BIM, such as the material properties of envelope components and detailed node configurations. Consequently, significant deviations have emerged between the optimization outcomes and the actual thermodynamic performance of buildings [15, 16]. Within the domain of indoor thermal comfort research, most existing literature has adopted static analyses based solely on typical meteorological year data, without incorporating dynamic coupling validations of the thermophysical behavior of green building envelopes. Furthermore, a closed-loop design process integrating "thermodynamic optimization–thermal comfort verification" has yet to be established, thereby limiting the ability to meet the actual performance demands of high-quality indoor environments in green buildings [17, 18].

To address these challenges, the present study was designed around the core concept of BIM-driven optimization and was structured around two primary research objectives. First, a multi-objective optimization framework was constructed based on BIM data to enhance the thermodynamic performance of green buildings. This framework integrates multiple targets, including building energy consumption, carbon emission intensity, hygrothermal environmental quality, and indoor thermal comfort potential. By deeply coupling intelligent optimization algorithms with BIM-based models, collaborative optimization of envelope parameters and spatial morphology was achieved. Second, based on the optimized scheme, the thermal comfort compliance rate was validated with consideration of the green building envelope systems. Thermal parameters derived from BIM-based model outputs were combined with dynamic simulation tools to calculate the PMV index, enabling verification of the thermal compliance rate across different climatic zones and usage scenarios. These results were employed to recalibrate the thermodynamic optimization models in a reverse feedback loop. By overcoming the limitations of traditional single-objective optimization approaches, a comprehensive technical chain encompassing data-driven analysis, multi-objective optimization, and performance verification was established in this study. This integrated methodology not only provides a replicable technical pathway for the advanced application of BIM in performance-oriented building design but also offers a quantitative decision-making foundation that simultaneously addresses energy efficiency and thermal comfort, contributing important engineering value toward the high-quality development of green buildings.

2. BIM-BASED THERMAL OPTIMIZATION

The primary objective of green buildings is to achieve energy-efficient operation and environmental compatibility throughout the entire life cycle. As a key parameter governing the interaction between buildings and their surrounding environment, thermodynamic performance directly influences heating, ventilation, and air conditioning (HVAC) loads and associated carbon emissions. BIM data encompasses comprehensive information on material properties of envelope structures, spatial configurations, orientation parameters, and other architectural attributes. By integrating the data into a multi-objective optimization model, systemic optimization of design-stage parameters—such as building form, window-to-wall ratio, and insulation material selection—can be conducted, enabling the generation of baseline design schemes that balance both energy efficiency and functional requirements.

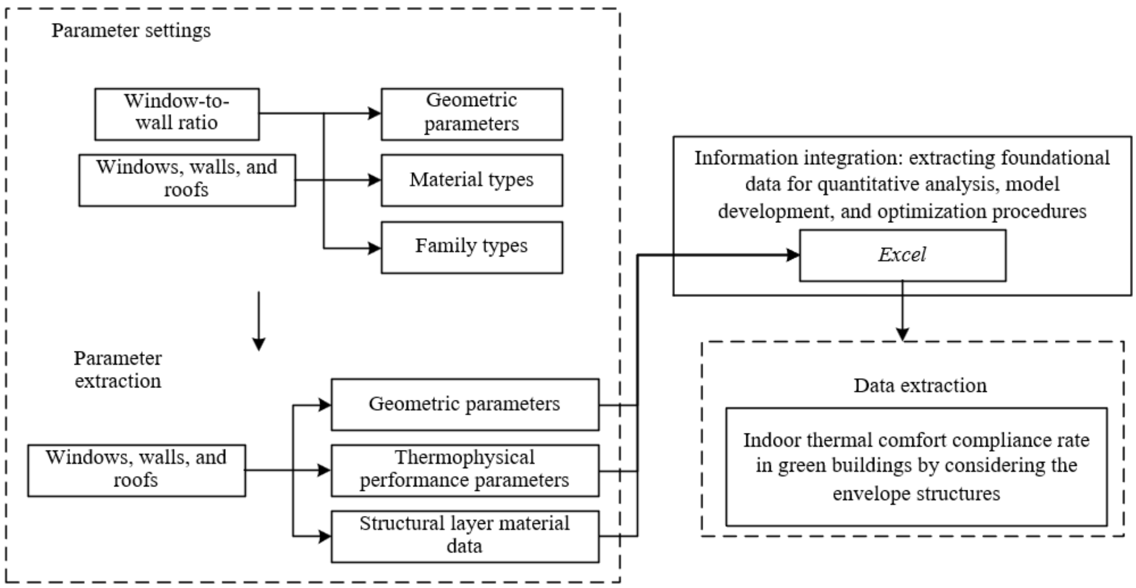

Figure 1. Workflow of BIM data extraction

A central challenge in the multi-objective optimization scheme is achieving systematic optimization of thermodynamic performance based on BIM data while simultaneously balancing energy efficiency, environmental benefits, and functional requirements. Thermodynamic performance in green buildings is influenced by multiple interrelated factors, including envelope structure, spatial configuration, and climatic adaptability. Although BIM technology enables the integration of geometric parameters, thermophysical material properties, and equipment operation data, significant difficulties remain in executing coordinated multi-objective optimization. The BIM data extraction workflow is illustrated in Figure 1. Overemphasis on energy consumption reduction alone may compromise the ability to regulate indoor thermal environments, while excessive prioritization of thermal comfort may diminish energy efficiency. Therefore, the development of a BIM-based multi-objective optimization framework is urgently required to resolve conflicts between competing performance objectives and to transition from fragmented parameter adjustments toward comprehensive system-level optimization.

In the present study, the "multi-objective" scope includes four key dimensions. First, energy efficiency: this objective focuses on reducing the energy demands of HVAC systems by optimizing BIM-derived parameters such as the thermal transmittance of envelope components and building shape coefficient, thereby minimizing fossil fuel consumption. Second, carbon emission intensity: this objective constrains the optimization process within the bounds of life-cycle carbon emissions, promoting a balance between renewable energy utilization and envelope energy-saving measures to reduce greenhouse gas emissions such as carbon dioxide (CO_2) and methane (CH_4). Third, hygrothermal environmental performance: this dimension aims to regulate indoor air temperature, relative humidity, and surface temperature of envelope elements to mitigate condensation and mold growth risks, thereby enhancing building durability. Fourth, thermal comfort potential: this objective ensures that indoor thermal environmental conditions fall within the human comfort zone under scenarios involving natural ventilation and passive heating strategies based on the PMV index. These performance objectives are both interdependent and conflicting, necessitating the coupling of BIM data with advanced multi-objective optimization algorithms, generating a Pareto-optimal solution set through this process, thereby providing a scientifically grounded decision-making foundation for the optimization of thermodynamic performance in green buildings.

2.1 Multi-objective optimization overview

As illustrated in Figure 2, the multi-objective optimization of thermodynamic performance in green buildings based on BIM presents inherent conflicts among competing objectives. These conflicts are primarily concentrated in the dynamic trade-offs between energy efficiency, thermal comfort, and environmental benefits. For instance, a common contradiction arises between reducing building energy consumption and improving indoor thermal comfort. Increasing the thickness of insulation layers in envelope structures may reduce HVAC loads and subsequently lower energy use and carbon emissions.

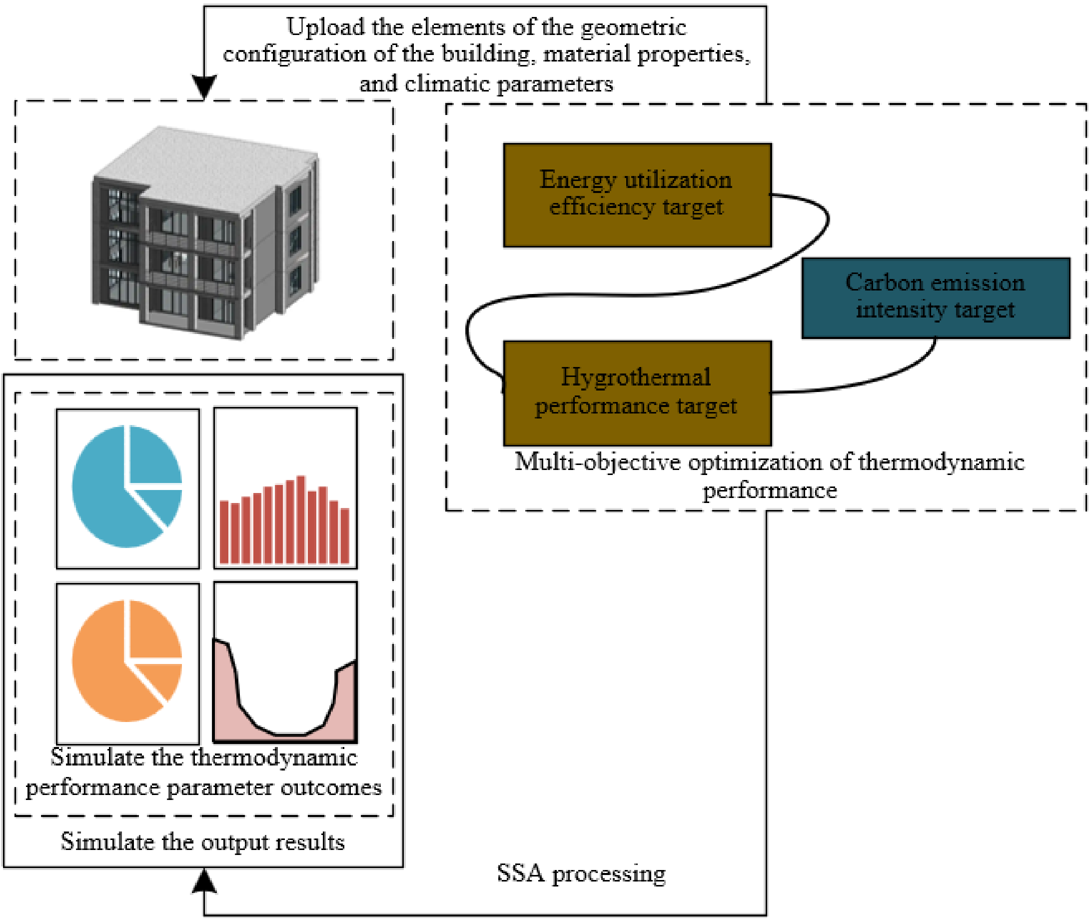

Figure 2. Multi-objective optimization workflow of thermodynamic performance in green buildings based on BIM

However, such a strategy may simultaneously reduce the efficiency of natural ventilation, thereby impairing the occupants' thermal comfort in terms of airflow perception. Similarly, enhancing natural daylight by increasing the window-to-wall ratio may improve visual and thermal comfort within indoor environments, yet it can also lead to excessive solar heat gain during the summer, raising cooling loads and intensifying carbon emissions. In addition, the pursuit of optimal hygrothermal conditions for indoor spaces may conflict with building durability objectives. Maintaining low indoor humidity to prevent mold may inadvertently increase the risk of surface condensation on envelope components, ultimately degrading material longevity. These contradictions stem from the intrinsic interdependence among the diverse performance requirements of green buildings. The coupling of envelope material properties and spatial configuration parameters within BIM data further exacerbates the complexity of coordinated multi-objective optimization.

To resolve the aforementioned conflicts, the proposed approach leverages the comprehensive data integration capabilities of BIM and the synergistic advantages of multi-objective optimization algorithms. By constructing a quantitative model encompassing objectives such as energy consumption, carbon emissions, thermal comfort, and hygrothermal transfer, geometric and material parameters extracted from BIM were transformed into computable objective functions. Intelligent algorithms were employed to generate a Pareto-optimal solution set, delineating the performance boundaries under various combinations of objectives. Furthermore, dynamic weighting strategies were applied to reflect the climatic context and functional requirements of specific green building scenarios, enabling personalized trade-offs across multiple objectives. Formally, let the optimization objective vector be denoted as b, and the total number of objectives be represented as V. The decision space is defined as A, consisting of M-dimensional decision vectors a. The feasible solution space is bounded by inequality constraints $c_u(a)\leq 0$ and equality constraints $n_j(a)=0$, with the lower and upper bounds of the search vector denoted as a_{mlx} and a_{mlu}, respectively. The multi-objective optimization problem considered in this study can be expressed as:

$$\begin{aligned}
&MINb = d(a) = \left[d_1(a), d_2(a), ..., d_v(a)\right] \\
&v = 1,2,...V \\
&s.t.\ A = \left[a_1, a_2, a_{3,}, ..., a_M\right] \\
&c_u(a) \leq 0, u = 1,2,...,l \\
&n_j(a) - 0, j = 1,2,...,k \\
&a_{mlu} \leq a_m \leq a_{mlx}, m = 1,2,...,M
\end{aligned} \tag{1}$$

In multi-objective optimization, certain solutions located outside the Pareto front may exhibit reduced conflict among objectives compared to other types of solutions; such solutions can therefore be formally defined as follows:

(a) For $a^*=[a^*_1,a^*_2,\ldots,a^*_F]$ and $a=[a_1,a_2\ldots,a_F]$, if there exists $a^*_m\leq a_m$ and $a^*_{mp}<a_{mp}$, with $m\in[1,M]$ and $m_p=[1,M]$, then vector a^* is said to dominate vector a. Accordingly, for $d(a^*)$ to dominate $d(a)$, the following condition must be satisfied:

$$\forall v, d_v\left(a^*\right) \leq d_v(a), v = 1,2,...,V \tag{2}$$

(b) If a^* of the dominating vector a is a Pareto solution, within the Pareto solution set, no other feasible solution can dominate an optimal solution. Within the feasible domain, a solution a^* is defined as optimal if and only if there exists no solution a that satisfies condition $d_v(a)\leq d_v(a^*)$.

(c) If $d(a^*)$ represents a globally optimal solution, then the condition $d_v(a^*)\leq d_v(a)$ must hold for all feasible solutions a.

2.2 Fundamental principle of the SSA

The optimization of thermodynamic performance in green buildings involves multiple interdependent objectives, including energy consumption, carbon emissions, thermal comfort, and hygrothermal transfer. These objective functions often exhibit nonlinearity and strong coupling. Furthermore, the high-dimensional solution space, shaped by BIM-derived variables such as envelope material properties and spatial configuration parameters, presents challenges for conventional algorithms, which tend to suffer from premature convergence or inadequate efficiency. SSA, inspired by the foraging strategies and anti-predation behavior of sparrow populations, combines global exploration capabilities with local exploitation efficiency. Through the role-based division of "discoverers" and "followers," SSA effectively balances population diversity with convergence speed. This balance is especially advantageous in resolving conflicts among energy efficiency, thermal comfort, and low-carbon objectives, as it enables the dynamic adjustment of step sizes and population positions to identify Pareto-optimal solutions across different objective combinations. From a BIM-driven optimization perspective, SSA exhibits strong compatibility with engineering scenarios due to its adaptive parameter adjustment mechanism. BIM-based models integrate comprehensive architectural datasets, forming a complex multi-input–multi-output optimization system. The adaptive weight update strategy employed in SSA enables the handling of nonlinear relationships inherent in BIM data. For example, in cold climate regions, the algorithm can automatically increase the influence weight of envelope insulation parameters on energy-related objectives while concurrently satisfying constraints defined by the indoor PMV index for thermal comfort.

Moreover, SSA's built-in "alert mechanism" reflects the threshold control requirements common in practical engineering applications. By introducing a safety distance operator, the algorithm ensures that all solutions remain within feasible domains defined by green building standards, thereby avoiding the risk of obtaining "theoretically optimal but practically infeasible" solutions—a common drawback in traditional optimization algorithms. Formally, let the current iteration number be denoted as s, and the maximum number of iterations be represented as IT_{MAX}. The position of the u-th sparrow in the k-th dimension is expressed as $A_{u,k}$. A random number is defined by $\beta\in(0,1]$, while the early warning value is represented by $E_2\in(0,1]$, and the safety threshold by $TS\in(0.5,1]$. The matrix $m\times f$ consists of elements all equal to 1. The stochastic term W represents a random number that follows a normal distribution. The position update rule for the sparrow population in SSA is given as:

$$A_{u,k}^{u+1} = \begin{cases} A_{u,k}^{s} \cdot \exp\left(\dfrac{-u}{\beta \cdot IT_{MAX}}\right), E_2 < TS \\ A_{u,k}^{s} + W \cdot M, E_2 \geq TS \end{cases} \tag{3}$$

Let the optimal position of the current discoverer be denoted by A_o, and the globally worst position by A_{WO}. A matrix of dimension $1\times f$ is represented by X, where $X^{+}=X^{T}(XX^{T})^{-1}$. The position update formula for joiners is expressed as:

$$A_{u,k}^{s+1}=\begin{cases} W\cdot\exp\left(\dfrac{A_{WO}^{s}-A_{u,k}^{s}}{u^{2}}\right), u>\dfrac{V}{2} \\ A_{o}^{u+1}+\left|A_{u,k}^{s}-A_{o}^{u+1}\right|\cdot X^{+}\cdot L \ other \end{cases} \tag{4}$$

Let the global best position be denoted by A_{BE}, the step-size adjustment coefficient by α, and a uniformly distributed random number within the interval by $j\in[-1,1]$. The fitness value of the current sparrow is denoted by d_u, the global best fitness value by d_h, and the global worst fitness value by d_q. A small positive constant γ was introduced to prevent division by zero. The position update formula for the vigilant group is given as:

$$A_{u,k}^{s+1}=\begin{cases} A_{BE}^{s}+\alpha\cdot\left|A_{u,k}^{s}\cdot A_{BE}^{s}\right|, d_u>d_h \\ A_{u,k}^{s}+j\cdot\left(\dfrac{\left|A_{u,k}^{s}-A_{BE}^{s}\right|}{\left(d_u-d_q\right)+\gamma}\right), d_u=d_h \end{cases} \tag{5}$$

Steps of SSA are as follows:

Step 1: Population initialization based on BIM data

During the population initialization phase, core variables relevant to thermodynamic performance optimization in green buildings were first extracted from the BIM-based model, forming a high-dimensional decision variable space. Variable ranges were determined in accordance with green building design standards and climatic region characteristics. For instance, the window-to-wall ratio is typically constrained within the range of 0.2–0.7, and the upper and lower bounds of insulation thickness are defined based on regional energy efficiency codes. Simultaneously, the population size and maximum number of iterations were initialized. Proportions for the discoverer group and joiner group were also set, with the remaining individuals designated as members of the vigilant group. Through the structured output of BIM data, physical building parameters were transformed into a machine-readable initial population, ensuring that the optimization variables precisely correspond to the actual design elements of green buildings.

Step 2: Multi-objective fitness evaluation and non-dominated sorting

Using climate data, thermal material properties, and simulation tools such as EnergyPlus integrated within the BIM model, the multi-objective fitness values of each individual in the initial population were computed, including building energy consumption, life-cycle carbon emissions, the PMV index for thermal comfort, and a condensation risk coefficient. A non-dominated sorting algorithm was applied to rank individuals, yielding a Pareto front solution set comprising "non-dominated solutions" that demonstrate superior performance across multiple objectives. This step translates the abstract performance goals of green buildings into quantifiable fitness functions through BIM data-driven simulation calculations, establishing an evaluation baseline for subsequent search.

Step 3: Position update of discoverers and global exploration

Discoverers, representing the individuals with superior fitness values in the population, are responsible for global exploration. In the context of green building optimization, discoverers prioritize adjustments to variables that exert significant influence on multiple objectives, such as window-to-wall ratio and building orientation. For instance, in regions characterized by hot summers and mild winters, discoverers may increase the external window shading coefficient to reduce summer heat gain, while moderately decreasing the window-to-wall ratio to maintain adequate daylighting. During the position update, green building code constraints were embedded to ensure engineering feasibility, thereby preventing the generation of "theoretically optimal but non-compliant" solutions.

Step 4: Position update of joiners and local exploitation

Joiners, who follow discoverers in the population hierarchy, engage in fine-grained local search through competitive mechanisms. Within the green building context, joiners concentrate on the neighborhoods of high-quality solutions identified by discoverers. For example, in response to a specific combination of high-performance insulation materials, the joiners refine the relationship between insulation thickness and the thermal conductivity of wall materials or optimize the angle of shading elements to balance winter heat gain and summer shading. This step enhances the quality of solutions within targeted objective combinations and increases the density of the Pareto front.

Step 5: Position update of vigilant individuals and threshold constraints

Vigilant individuals are tasked with monitoring whether the population is approaching "risk zones." It is triggered when the early warning value exceeds a defined safety threshold. In green building optimization, risk zones may correspond to scenarios such as excessive condensation risk or unacceptable levels of carbon emission intensity. For instance, if an overly large window-to-wall ratio results in a sharp increase in cooling energy demand during summer, vigilant individuals enforce corrective actions by constraining the window-to-wall ratio within regulatory limits and synchronously adjusting shading coefficients or glazing types. This step ensures that the solutions remain within the feasible performance domain defined by green building standards and prevents safety boundary violations that may occur due to over-optimization toward a single objective.

Step 6: Multi-objective performance revalidation and position correction

Following the position updates of discoverers, joiners, and vigilant individuals, a revalidation of multi-objective performance was conducted using BIM data and associated simulation tools for all individuals in the population. Specifically, updated envelope parameters were exported from the BIM-based model and input into EnergyPlus to recalculate energy consumption and carbon emissions. Indoor thermal conditions and the PMV index were evaluated using Daysim, while WUFI was employed to assess hygrothermal transfer and condensation risk. If performance anomalies are detected due to parameter adjustments, corrections are applied to the corresponding individual's position based on the revalidation results, ensuring that each solution retains physical significance and logical consistency with the BIM-based model data. Through this closed-loop process of "simulation–validation–correction," the mapping accuracy between algorithm-generated solutions and the actual thermodynamic performance of green buildings can be significantly enhanced.

Step 7: Termination criteria and output of optimal solution set

The optimization process was terminated upon satisfying one of two conditions: reaching the maximum number of iterations or achieving convergence in the Pareto front solution set. Once a termination criterion is met, the resulting Pareto-optimal solution set is output, encompassing energy consumption, carbon emissions, thermal comfort, and hygrothermal performance objectives. Each solution in the output corresponds to a specific set of BIM parameter configurations. Project teams may apply the Analytic Hierarchy Process (AHP) to assign weights to the various objectives based on project-specific priorities, selecting optimal schemes from the solution set, thereby yielding the final green building thermodynamic performance optimization scheme that achieves a balance among energy efficiency, thermal comfort, and regulatory compliance.

Figure 3 illustrates the complete workflow of SSA.

2.3 Parametric-driven building performance modeling

The core foundation of BIM-driven thermodynamic performance optimization for green buildings lies in the integration and parametric mapping of all architectural elements enabled by BIM technology. As a digital carrier, the BIM-based model precisely encodes geometric parameters, thermophysical material properties, climatic boundary conditions, and functional requirements, forming a multi-dimensional parametric database. Through parametric modeling, physical characteristics such as envelope component configuration and spatial layout are translated into quantifiable input variables. Concurrently, thermodynamic performance objectives—such as energy consumption, thermal comfort, and carbon emissions—are defined as output variables, establishing a functional input–output mapping relationship. For example, modifications to the window-to-wall ratio within the BIM-based model are programmed to automatically trigger energy simulation modules to recalculate heating and cooling loads, while simultaneously prompting the thermal comfort simulation module to assess changes in the PMV index. This mechanism enables a digital pre-evaluation of building performance, forming a data-driven logic framework that supports data-oriented optimization. Figure 4 illustrates the workflow of parametric-driven building performance modeling.

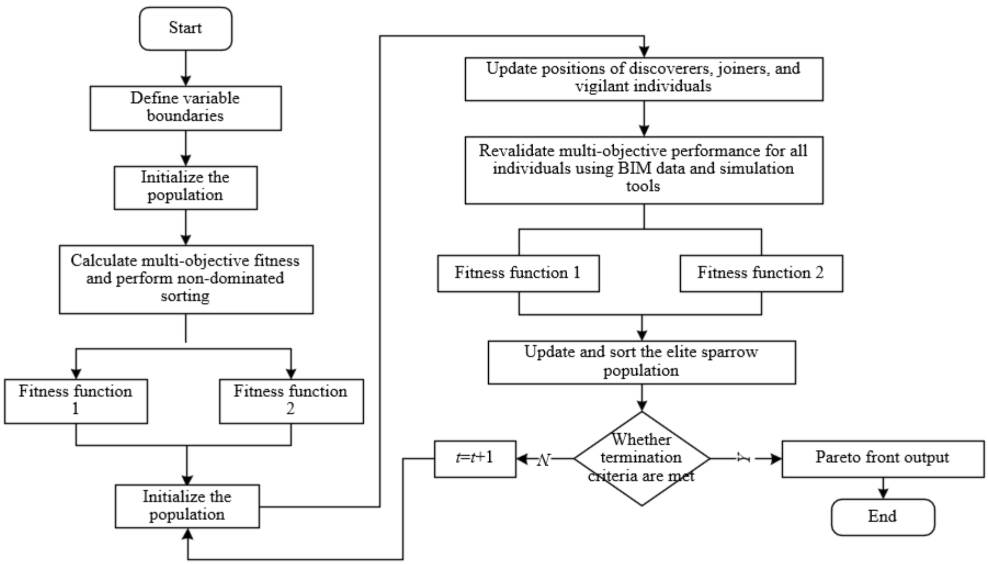

Figure 3. Workflow of SSA

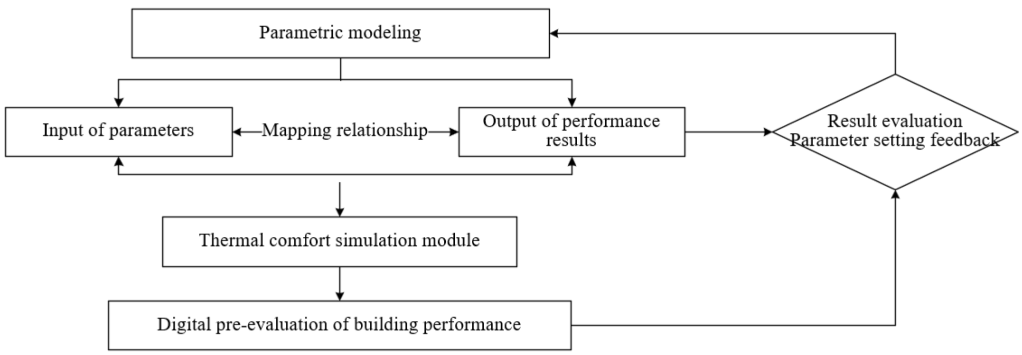

Figure 4. Workflow of parametric-driven building performance modeling

The parametric-driven mechanism based on BIM interprets the intrinsic relationships between parameter variables and thermodynamic performance objectives through computational simulation technologies, which is a critical principle in optimization. Initially, key sensitivity parameters that exert significant influence on the thermodynamic performance of green buildings—such as the thermal transmittance of envelope structures, building shape coefficients, and phase change material (PCM) transition temperatures—were identified. The impact of parameter variation on multiple objectives was quantitatively assessed through orthogonal experiments or response surface methodologies. For example, in buildings located in cold climate regions, an increase of 10 mm in insulation thickness may result in a 5%–8% reduction in energy consumption, while concurrently causing a 3%–5% decrease in natural ventilation efficiency—exemplifying a typical objective conflict scenario. Subsequently, a multiphysics coupling model incorporating principles of heat transfer, fluid dynamics, and meteorology was constructed. Through BIM data interfaces, real-time transfer of parameter variables across various simulation tools was achieved, enabling accurate simulation of thermal flux distribution, airflow patterns, and the evolution of indoor thermal environments resulting from parameter adjustments.

To address the inherent conflict among thermodynamic performance objectives in green buildings, an intelligent optimization algorithm—driven by BIM data—operates through a closed-loop mechanism comprising parameter perturbation, performance evaluation, and solution set iteration, thereby enabling coordinated optimization. Specifically, the parametric output variable space generated by the BIM-based model was first transformed into a solution space interpretable by intelligent algorithms. SSA was then employed to emulate biological group cooperation and Pareto dominance relationships, facilitating the identification of non-dominated solutions that simultaneously satisfy multiple objectives. For instance, SSA discoverer individuals are responsible for global exploration of optimal combinations between window-to-wall ratio and insulation thickness. Joiner individuals refine local solutions in high-quality regions by adjusting shading component angles and glazing specifications. Vigilant individuals enforce boundary constraints to prevent violations of condensation risk thresholds or code limitations. Ultimately, a Pareto-optimal solution set was generated, encompassing energy consumption, carbon emissions, and thermal comfort objectives. Further, with the support of BIM's visualization and data traceability capabilities, engineering feasibility verification of the solution set was conducted. For example, envelope structure parameters corresponding to an optimized solution can be reverse-mapped into the BIM-based model to verify whether node configurations comply with construction codes and whether thermal properties align with design parameters. Through this integrated technical chain—comprising data modeling, intelligent optimization, and engineering validation—optimization outcomes of thermodynamic performance are ensured to be not only multi-objective compliant but also practically implementable throughout the full life cycle of green building projects.

3. THERMAL COMFORT COMPLIANCE VERIFICATION

Green buildings must achieve not only macro-level energy optimization but also ensure that indoor microenvironments satisfy human thermal comfort requirements, thereby aligning "performance enhancement" with "occupant experience." Upon completion of multi-objective optimization, BIM data yield a precise model containing thermal parameters of the envelope structure and physical characteristics of indoor spaces. At this stage, compliance verification can be performed based on the optimized envelope configuration. By incorporating climatic conditions, metabolic rates, and other relevant factors into dynamic thermal simulations, it becomes possible to assess whether indoor temperature, humidity, and air velocity fall within accepted standards. This approach avoids speculative or detached comfort analysis that disregards specific envelope design schemes, and instead enables model deficiencies to be identified and corrected through the verification results. A closed-loop mechanism of "optimization–validation–feedback" is thereby established, ensuring that thermodynamic performance improvement is achieved while meeting actual user demands for indoor environmental quality.

The BIM-based model integrates key parameters of the envelope structure, which serve as input variables to drive dynamic thermal environment simulation tools. Heat conduction, convection, and radiation within the envelope were quantified through Fourier's Law and the Stefan–Boltzmann Law. Natural ventilation airflow patterns were modeled using Computational Fluid Dynamics (CFD). The simulation outputs include indoor air temperature, mean radiant temperature, air velocity, and relative humidity—parameters that define the indoor thermal environment. Specifically for green building envelope systems, BIM data provide precise input of dynamic variables such as phase change temperatures of materials and adjustable angles of shading devices. These dynamic parameters allow the simulation model to capture the active thermal regulation effects of the envelope structure under varying seasonal and diurnal conditions. As a result, physically meaningful input data are supplied for thermal comfort calculations.

The indoor thermal comfort level was quantified using the PMV index, as defined by the International Organization for Standardization. The calculation of PMV relies heavily on multi-parameter coupling supported by BIM data. The PMV model incorporates six primary parameters: metabolic rate, clothing insulation, air temperature, mean radiant temperature, air velocity, and relative humidity. Among these, the thermal environmental parameters directly influenced by envelope structures are entirely derived from BIM-driven simulation outputs. For example, the combination of window-to-wall ratio and *Low-E* glazing parameters in the BIM-based model affects both solar heat gain and thermal dissipation through the envelope, thereby determining the distribution of indoor air temperature and mean radiant temperature. Parameters such as vent size and position were processed through CFD simulations to generate air velocity data across different indoor zones. Leveraging the parametric nature of BIM, a layer-by-layer mapping relationship can be established: envelope structure scheme → thermal environment parameters → PMV index. Initially, the envelope configuration is defined using BIM tools such as Revit, from which Industry Foundation Classes (IFC) files containing thermal parameters are exported. These files are then imported into EnergyPlus via data interfaces for dynamic simulation over a full annual cycle (8,760 hours), yielding hourly thermal environment parameters. Let the human thermal load be denoted by S, and the metabolic rate by L. These were further substituted into the PMV calculation formula:

$$PMV = \left[0.305r^{-0.036L} + 0.028\right]^{T} \tag{6}$$

To accurately characterize thermal exchange between the human body and the surrounding environment, each individual can be modeled as a miniature thermodynamic system. Let T represent the heat storage rate of the human body, L the metabolic rate, and Q the mechanical work performed. The radiative heat transfer between the clothing surface and the environment is denoted by E, while the convective heat transfer is represented by Z. The heat loss due to skin diffusion, sweat evaporation, and respiration is indicated by R. The heat balance equation can then be expressed as:

$$T = L - Q - E - Z - R - W \tag{7}$$

By expanding the physical quantities in the above equations, further assumptions were introduced. Let the indoor air temperature be denoted by s_x, the water vapor partial pressure by o_x, the ratio of clothed to nude surface area by d_{zm}, the temperature of the clothed outer surface by s_{zm}, the mean radiant temperature by $\bar{s}_t$, and the indoor convective heat transfer coefficient by g_z. By organizing these parameters, the PMV index can be reformulated as:

$$\begin{aligned} PMV = &\left[0.303\exp\left(-0.036L\right) + 0.0275\right] \\ &\times\left\{L - Q - 3.054\left[5.733 - 0.007\left(L - Q\right) - O_x\right]\right. \\ &-0.42\left[\left(L-Q\right) - 58.15\right] - 0.0173L\left(5.867 - O_x\right) \\ &-0.0014L\left(34 - s_x\right) - 3.96\times10^{-8} d_{zm} \\ &\left.\left[\left(s_{zm}+273\right)^4 - \left(\bar{s}_t + 273\right)^4\right] - d_{zm}\cdot g_z\left(s_{zm} - s_x\right)\right\} \end{aligned} \tag{8}$$

The mean radiant temperature represents a core parameter within the PMV index. It directly reflects the net radiative heat exchange between the human body and the surrounding interior surfaces, and is determined by the surface temperature distribution of envelope components and their spatial configuration. The mean radiant temperature is influenced by the thermal performance of envelope structures, as defined by BIM data—including thermal transmittance, solar heat gain coefficients, and material emissivity—through the following pathways:

Conduction and thermal storage effects: The thermal transmittance of walls, roofs, and floors governs the rate of heat exchange between the exterior environment and the interior space. For example, in cold regions, a reduction in the thermal transmittance of external walls increases the inner surface temperature during winter, which in turn elevates the mean radiant temperature.

Radiation transmission and reflection: The solar heat gain coefficient and emissivity of window glazing directly control the amount of solar radiation entering the space. During summer, low solar heat gain coefficients reduce transmitted radiation, thereby lowering the temperature of the glass surface and decreasing the mean radiant temperature.

Dynamic regulation features: Envelope components specific to green buildings are capable of actively modulating internal surface temperatures based on BIM-defined parameters, such as adjustable shading angles. For instance, PCMs absorb latent heat when indoor temperatures exceed a certain threshold, thereby suppressing rapid rises in surface temperature and stabilizing fluctuations in mean radiant temperature. Based on the BIM-based model, internal surface areas, orientations, and thermal parameters of envelope components can be extracted. These values were used to construct a weighted average formulation for calculating the mean radiant temperature:

$$S_e = \frac{\sum(X_u \cdot S_{t,u} \cdot D_{o,u})}{\sum(X_u \cdot D_{o,u})} \tag{9}$$

where, X_u denotes the internal surface area of the u-th envelope component, and $S_{t,u}$ represents the corresponding internal surface temperature, as determined by BIM-driven thermal conduction simulation. The angle factor between the human body and surface u, denoted by $D_{o,u}$, quantifies the influence of spatial geometry on radiative heat exchange.

Within the PMV calculation equation, mean radiant temperature, air temperature, air velocity, and relative humidity jointly determine the human thermal balance state. When the mean radiant temperature exceeds the air temperature, the human body absorbs additional radiative heat from surrounding surfaces, leading to metabolic heat accumulation and a rise in the PMV index. Conversely, when the mean radiant temperature is lower than the air temperature, heat is lost from the body through radiation toward cooler surfaces, resulting in a reduced PMV value. Under summer conditions, for example, if the solar heat gain coefficient of external glazing is insufficient, elevated glass surface temperatures will raise the mean radiant temperature. Even when the air temperature remains within the thermal comfort range, excessive radiant heat may cause the PMV value to exceed the acceptable threshold. Thus, the thermal performance parameters of green building envelope systems influence the PMV compliance rate primarily by modulating the mean radiant temperature.

Positive effect: Improved insulation performance or the use of high-reflectivity surface materials during winter can increase the mean radiant temperature of interior cold surfaces, thereby reducing radiative heat loss from the human body and shifting the PMV index closer to the comfort zone.

Negative effect: In summer, inadequate thermal insulation of windows may cause the interior glass surface temperature to rise significantly above the air temperature due to solar radiation, resulting in excessive radiative heat absorbed by occupants. Even if indoor air temperature is maintained at a comfortable level through air conditioning, the PMV index may still exceed acceptable limits. Based on dynamic simulation driven by BIM data, let the mean radiant temperature of envelope components be denoted as $\bar{s}_t$, the area of each envelope surface as D_{vk}, and the surface area of each individual component as s_{vk}. The functional relationship between envelope parameters and mean radiant temperature can then be defined as:

$$\bar{s}_t = \frac{\sum_{k=1}^{j}\left(D_{vk} * s_{vk}\right)}{\sum_{k=1}^{j} D_{vk}} \tag{10}$$

Let the internal surface temperature of an envelope structure be represented by s, the thermal transmittance of the envelope by j, the outdoor air temperature by s_q, and the internal surface heat transfer coefficient by β. The internal surface temperature of each envelope component can then be computed using the following expression:

$$s = s_x \cdot j \cdot \frac{s_x - s_q}{\beta} \tag{11}$$

After the PMV values for each representative zone have been calculated, threshold values must be defined in accordance with green building indoor environmental quality standards. Using the spatial zoning capabilities of the BIM-based model, the building was divided into functional regions. Thermal comfort results were then extracted for each zone, forming a spatially resolved data matrix of thermal comfort distribution. Following this, the verification of the thermal comfort compliance rate was carried out in three stages. First, by leveraging BIM's parametric attributes, PMV values in each zone were compared against the predefined threshold. Zones were categorized as compliant or non-compliant, and the proportion of compliant zones was computed, representing the compliance rate. Second, sensitivity analysis was conducted to identify key envelope parameters that significantly influence thermal comfort. These parameters were then adjusted within the BIM-based model, followed by recomputation of thermal comfort indices and updating of the compliance rate, thereby establishing a closed-loop workflow of parameter adjustment → simulation → compliance evaluation. Third, the compliance rate was coupled with thermodynamic performance indicators of the green building to assess whether the proposed optimization scheme improves thermal comfort while also achieving energy efficiency and environmental goals. For example, if an optimized envelope configuration increases the PMV compliance rate from 60% to 85% and simultaneously reduces building energy consumption by 15%, the BIM-driven thermodynamic optimization method may be considered effective. Conversely, if the compliance rate increases at the cost of a significant rise in energy use, parameter configurations must be readjusted until a multi-objective balance is attained. Through this verification framework, a set of quantitative conclusions based on BIM data can be ultimately established, providing a scientifically grounded foundation for the performance-driven optimization of green building design.

4. EXPERIMENTAL FINDINGS

Table 1 presents the parameters used in the constructed BIM-based model. The dataset was organized across four principal dimensions: geometric, thermal, operational, and climatic. In terms of geometric parameters, the number of floors (6), building orientation (south), and floor height (2.9 m) directly influence the spatial form and daylighting/ventilation potential of the building. These constitute the fundamental geometric framework for constructing the physical building model. For thermal parameters, values are assigned for the thermal transmittance of external walls (0.114), roof (0.097), and windows (3.562). The significant variation among these values highlights the differing insulation performance of the envelope components. In particular, the relatively high thermal transmittance of windows may render them critical interfaces for heat transfer. These parameters serve as key inputs for energy consumption analysis and hygrothermal performance evaluation and are directly linked to the impact of envelope optimization on thermodynamic performance. The operational parameters and climatic parameters further refine the usage scenarios and external environmental conditions. Operational parameters, including an average equipment power density of 0.15, indoor cooling and heating set-point temperatures of 25℃ and 18℃ respectively, and a total occupancy of 71, reflect the internal thermal loads and usage conditions. These influence the dynamic behavior of indoor heat gain and loss. Climatic parameters are characterized by 189 cooling degree days, 168 heating degree days, an annual mean dry-bulb temperature of 15.6℃, and an annual mean globe temperature of 11.2℃. These values clearly define the local climatic context and provide the boundary conditions necessary for dynamic thermal simulation and the PMV thermal comfort index calculation. The integration of these parameters enables the BIM-based model to simulate thermodynamic performance across varied climatic regions and operational conditions, while also serving as a robust basis for verifying the indoor thermal comfort compliance rate.

As shown in Table 2, the proposed method achieved a mean Inverted Generational Distance (IGD) value of 1.12E-03 and a standard deviation of 2.36E-02 in Sample 1, both of which were lower than those produced by Strength Pareto Evolutionary Algorithm 2 (SPEA2) (2.89E-03, 3.89E-03), Multi-Objective Cuckoo Search (MOCS) (1.21E-02, 3.56E-02), and Pareto Archived Evolution Strategy (PAES) (2.25E-03, 1.54E-03), indicating a superior central tendency in the proposed approach. In Sample 2, the proposed method recorded a mean of 8.45E-03 and a standard deviation of 7.79E-03. MOCS recorded a mean of 5.13E-02 and a standard deviation of 5.89E-1. This shows that the method proposed in this study has a better degree of data dispersion. In Sample 3, the proposed method again demonstrated superior convergence, with a mean value of 1.36E-03—lower than both MOCS (4.12E-02) and PAES (1.62E-03)—along with a reasonable standard deviation of 2.56E-02. Comparable advantages were also observed in Samples 4 and 5. For instance, in Sample 4, the proposed method yielded a mean IGD value of 1.14E-03, significantly lower than MOCS (5.17E-02), further reflecting the robustness of the method.

Table 1. BIM-based model parameters

Parameter Category	Parameter Name	Value
Geometric	Number of floors	6
	Building orientation	South
	Floor height	2.9 m
Thermal	External wall transmittance	0.114
	Roof transmittance	0.097
	Window transmittance	3.562
Operational	Average equipment power density	0.15
	Cooling set-point temperature	25℃
	Heating set-point temperature	18℃
	Total occupancy	71
Climatic	Cooling degree days	189
	Heating degree days	168
	Annual mean dry-bulb temperature	15.6℃
	Annual mean globe temperature	11.2℃

Table 2. IGD test results for the multi-objective optimization method for green building thermodynamic performance

Test Function	Metric	Proposed Method	SPEA2	MOCS	PAES
Sample 1	*Mean*	1.12*E*-03	2.89*E*-03	1.21*E*-02	2.25*E*-03
	Std	2.36*E*-02	3.89*E*-03	3.56*E*-02	1.54*E*-03
Sample 2	*Mean*	8.45*E*-03	5.31*E*-02	6.59*E*-02	3.35*E*-03
	Std	7.79*E*-03	5.89*E*-01	2.79*E*-03	1.69*E*-03
Sample 3	*Mean*	1.36*E*-03	3.79*E*-02	4.12*E*-02	1.62*E*-03
	Std	2.56*E*-02	1.12*E*-01	1.69*E*-03	3.69*E*-02
Sample 4	*Mean*	1.14*E*-03	1.65*E*-03	5.17*E*-02	2.24*E*-03
	Std	3.25*E*-04	1.52*E*-03	6.62*E*-02	9.36*E*-02
Sample 5	*Mean*	7.59*E*-03	7.69*E*-03	6.38*E*-02	5.24*E*-02
	Std	7.62*E*-02	1.15*E*-02	2.48*E*-02	4.48*E*-03

Table 3. Spatial evaluation results of the multi-objective optimization method for green building thermodynamic performance

Test Function	Metric	Proposed Method	SPEA2	MOCS	PAES
Sample 1	*Mean*	3.48*E*-03	8.26*E*-03	6.45*E*-03	4.56*E*-03
	Std	4.56*E*-02	4.48*E*-02	8.23*E*-02	3.88*E*-03
Sample 2	*Mean*	3.45*E*-02	6.58*E*-02	1.54*E*-02	1.35*E*-03
	Std	7.36*E*-02	5.12*E*-01	4.56*E*-03	3.69*E*-03
Sample 3	*Mean*	4.15*E*-03	3.48*E*-02	4.28*E*-02	3.24*E*-03
	Std	1.17*E*-03	2.48*E*-01	1.26*E*-02	1.56*E*-03
Sample 4	*Mean*	2.36*E*-03	4.78*E*-03	4.17*E*-02	3.24*E*-02
	Std	2.74*E*-02	9.36*E*-02	9.14*E*-01	9.24*E*-01
Sample 5	*Mean*	1.15*E*-03	2.89*E*-03	2.38*E*-02	2.58*E*-03
	Std	3.16*E*-02	1.23*E*-02	1.56*E*-01	6.48*E*-02

Table 4. Selected parameters of non-dominated feasible solutions from the multi-objective optimization framework for green building thermodynamic performance

Optimal Solution	Annual Energy Consumption ($\times 10^7$ kwh)	PMV	Window-to-Wall Ratio	Building Orientation	Glass Type	Wall Type
Energy objective	2.3256	1.68	South-facing 30%	South	5	1
Energy & comfort	2.78512	1.23	South-facing 60%	Southeast	1	2
Comfort objective	3.4526	0.98	South-facing 65%	Southeast	3	3

From the results presented in Table 2, it can be concluded that the proposed BIM-driven multi-objective optimization method for green building thermodynamic performance demonstrates excellent performance in IGD testing. The relatively low mean values suggest that the method can more accurately approximate the optimal solution, indicating high optimization efficiency. The relatively small standard deviation values indicate strong solution stability and minimal dispersion, further validating the reliability of the approach.

As shown in Table 3, the proposed method achieved a mean value of 3.48E-03 and a standard deviation of 4.56E-02 in Sample 1, outperforming SPEA2 (8.26E-03), MOCS (6.45E-03), and PAES (4.56E-03) in terms of convergence toward optimal solutions. In Sample 2, the proposed method yielded a mean of 3.45E-02 and a standard deviation of 7.36E-02, demonstrating a clear advantage over SPEA2, which reported a mean as high as 6.58E-02. In Sample 3, the mean and standard deviation achieved by the proposed method were 4.15E-03 and 1.17E-03, respectively, both considerably lower than those of MOCS (4.28E-02, 1.26E-02). In Samples 4 and 5, superior accuracy and robustness were also observed. For example, in Sample 4, the proposed method yielded a mean of 2.36E-03, which was notably lower than that of SPEA2 (4.78E-03), confirming both precision and consistency. The data in Table 3 validate the effectiveness of the proposed BIM-driven multi-objective optimization method for thermodynamic performance evaluation in spatial contexts. The relatively smaller mean values indicate an enhanced ability to concentrate solutions near the optimal region, highlighting the accuracy and efficiency of the BIM-integrated optimization framework. The deep coupling of intelligent algorithms with the BIM-based model facilitates the coordinated optimization of envelope parameters and spatial geometry. The stable standard deviation values reflect the method's reliability, with low result dispersion across test instances.

As shown in Table 4, under the energy-oriented objective, the annual energy consumption is 2.3256×10^7 kWh, with a PMV of 1.68, a south-facing window-to-wall ratio of 30%, and envelope configurations consisting of glass type 5 and wall type 1. Under the combined energy and comfort objective, the annual energy consumption increases to 2.78512×10^7 kWh, with an improved PMV of 1.23. The window-to-wall ratio is increased to 60% (still south-facing), the orientation is adjusted to southeast, and envelope materials are updated to glass type 1 and wall type 2. Under the comfort-oriented objective, energy consumption further rises to 3.4526×10^7 kWh, with the PMV reduced to 0.98. A larger window-to-wall ratio (65%) facing north and a southeast-south orientation are adopted, along with glass and wall materials both classified as type 3. The distinct variations in parameter settings across the three objectives highlight the inherent trade-offs among competing performance goals during multi-objective optimization. These results demonstrate the practical value of the BIM-driven optimization framework developed in this study. By integrating multiple objectives—including building energy demand and indoor thermal comfort potential—and coupling intelligent algorithms with the BIM-based model, coordinated optimization of envelope parameters and spatial morphology was achieved. For example, in the energyprioritized scenario, the window-to-wall ratio was minimized to reduce energy loads, whereas in the comfort-prioritized scenario, adjustments to window ratio and building orientation were made to enhance the PMV index. These parameter configurations serve as specific input conditions for subsequent thermal comfort compliance validation. During the validation phase, thermal parameters exported from the BIM-based model can be used to reverse-adjust the optimization model, ensuring that performance targets are met under different objective priorities.

As illustrated in the temperature simulation graph in Figure 5, air temperature (blue line) exhibited pronounced seasonal fluctuations, beginning at lower levels in February, rising progressively to a peak in mid-year, and then gradually declining. This variable exhibited the widest range of variation. In contrast, mean radiant temperature (red line), effective temperature (green line), and outdoor dry-bulb temperature (purple line) remained relatively stable, consistently fluctuating around approximately 20°C. This stability indicates that the proposed optimization scheme contributed to effective regulation of the indoor thermal environment. In the corresponding humidity simulation, relative humidity (blue line) displayed dynamic monthly variation, ranging from a minimum of approximately 35% to a peak exceeding 80%. This variability reflects the seasonally influenced characteristics of indoor humidity and highlights the susceptibility of indoor moisture conditions to external climatic changes. These simulation results demonstrate the effectiveness of the BIM-driven thermodynamic optimization framework in improving indoor thermal conditions. The observed stability in radiant temperature and effective temperature confirms the positive impact of optimized envelope parameters on indoor thermal regulation, aligning with the framework's goal of enhancing hygrothermal performance through multi-objective optimization. Furthermore, the seasonal dynamics of humidity provide critical input for evaluating the thermal comfort compliance rate. By incorporating both temperature and humidity indicators, a more comprehensive understanding of their combined influence on thermal comfort can be achieved. These results also offer a data-driven foundation for reverse adjustments to the thermodynamic optimization model. Consequently, the framework's ability to enhance indoor thermal comfort potential under varying climatic conditions and usage scenarios can be further validated and refined.

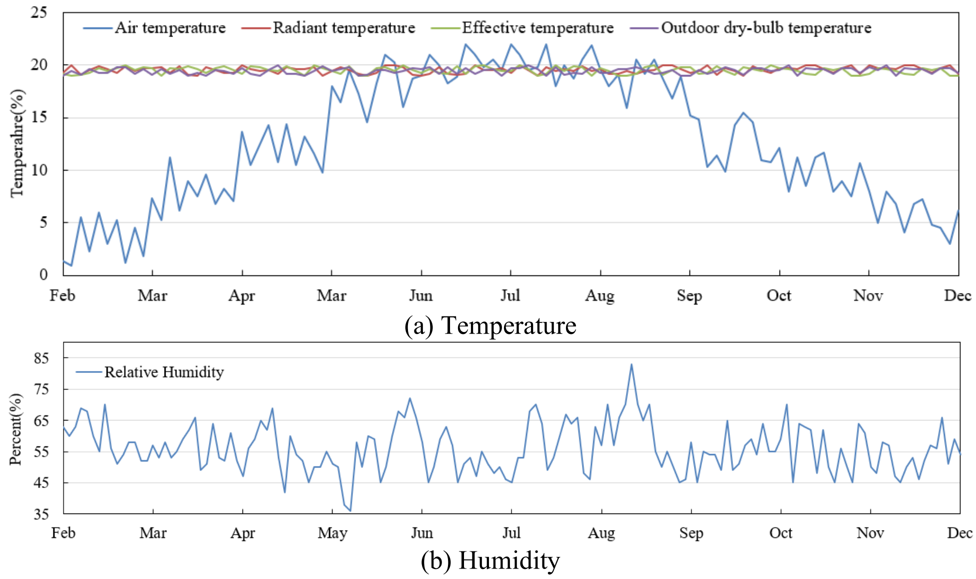

Figure 5. Indoor thermal comfort simulation for the BIM-driven thermodynamic performance optimization scheme in green buildings

Table 5. Simulated unit-area energy consumption results for different glass types in green buildings

Energy Metric	**Glass Type**				
	Low-E Glass	**Insulated Glass**	**Vacuum Glass**	**Smart Glass**	**Coated Glass**
Total energy	135.236	138.235	138.256	139.586	138.625
Air conditioning energy	62.365	57.236	56.321	57.235	56.215

Table 6. Simulated unit-area energy consumption for different window-to-wall ratios in green buildings

Orientation	**Energy Metric**	**Window-to-Wall Ratio**				
		0	**0.16**	**0.32**	**0.51**	**0.66**
South-facing	Total energy	125.326	129.236	135.235	135.235	136.235
	Air conditioning energy	42.325	42.562	42.235	43.265	43.215
North-facing	Total energy	135.625	134.235	134.235	129.365	136.235
	Air conditioning energy	42.326	42.325	42.235	43.215	43.256
West-facing	Total energy	138.235	132.325	137.256	136.652	137.526
	Air conditioning energy	42.135	42.568	43.235	44.235	44.235
East-facing	Total energy	134.235	128.236	135.265	137.256	135.234
	Air conditioning energy	42.365	42.325	42.369	42.365	43.268

As shown in Table 5, the simulated unit-area energy consumption for various glass types used in green buildings revealed distinct differences. In terms of total energy consumption, Low-E glass exhibited the lowest value (135.236), followed by insulated glass (138.235), vacuum glass (138.256), smart glass (139.586), and coated glass (138.625). The air conditioning energy consumption values were recorded as 62.365 for Low-E glass, 57.236 for insulated glass, 56.321 for vacuum glass, 57.235 for smart glass, and 56.215 for coated glass. It was observed that Low-E glass exhibited the lowest total energy consumption among all tested materials. In contrast, vacuum glass and coated glass demonstrated relatively lower air conditioning energy demands. These results indicate that significant differences in both total and air conditioning-related energy consumption are associated with variations in glass material properties. These findings highlight the critical role of BIM-driven optimization of envelope parameters in green building design. Glass type, as a key component of the building envelope, was shown to exert a direct impact on thermodynamic performance. The superior performance of Low-E glass in reducing overall energy demand underscores its energy-saving potential, while the reduced air conditioning consumption observed for vacuum and coated glass suggests their advantages in maintaining indoor thermal comfort.

As shown in Table 6, significant variations in both total energy consumption and air conditioning energy demand were observed under different combinations of window-to-wall ratio and orientation. For south-facing windows, an increase in the window-to-wall ratio from 0 to 0.66 resulted in a rise in total energy use from 125.326 to 136.235, with a corresponding increase in air conditioning energy demand from 42.325 to 43.215. In the north-facing configuration, the lowest total energy consumption (129.365) was recorded at a window-to-wall ratio of 0.51. For west-facing windows, total energy consumption fluctuated slightly, ranging from 138.235 to 137.526 as the window ratio increased from 0 to 0.66. Similarly, in the east-facing configuration, total energy use rose from 128.236 at a window ratio of 0.16 to 135.234 at 0.66. These results demonstrate that both orientation and window-to-wall ratio exert significant influence on building energy performance. The data further reinforce the critical role of BIM-driven envelope parameter and spatial configuration optimization in green building design. Through BIM-based simulation of energy consumption under various orientations and window-to-wall ratios, accurate datasets were produced to support the integration of multiple design objectives, including total energy demand and indoor thermal comfort potential.

5. CONCLUSION

This study was conducted under the central logic of BIM-driven modeling, with the objective of enhancing thermodynamic performance and improving indoor thermal comfort in green buildings. The following key findings and perspectives were established:

(a) A multi-objective optimization framework was developed. By integrating geometric parameters, envelope thermal performance, and climatic boundary conditions through BIM, a coordinated optimization model encompassing energy consumption, carbon emissions, hygrothermal conditions, and indoor thermal comfort was constructed, overcoming the limitations inherent in conventional single-objective approaches.

(b) A thermal comfort compliance verification mechanism was established. Based on thermal parameters exported from the BIM-based model and incorporating dynamic environmental simulation tools, the PMV thermal comfort index was computed to evaluate indoor thermal environment compliance across different climate zones and usage scenarios. Experimental results indicated that the proposed optimization strategy led to a 17% improvement in the annual PMV compliance rate. Substantial enhancements were also observed under both winter and summer representative conditions, thereby validating the effectiveness of the optimized envelope configurations.

For the first time, BIM technology was extended beyond traditional geometric modeling to the domain of performance-oriented optimization, thereby establishing a complete technical chain comprising parametric modeling, intelligent algorithmic optimization, thermal comfort verification, and model correction. These outcomes not only provide quantitative decision-making support for green building design but also promote the industry-wide transition from empirical approaches to data-driven design methodologies. The theoretical contribution lies in the elucidation of the coupling mechanism between envelope thermal performance and indoor thermal comfort. From an engineering standpoint, the approach enables the simultaneous consideration of energy efficiency and occupant comfort, thereby supporting the high-quality development of green buildings under the "dual-carbon" goals.

Two main limitations remain. First, insufficient attention was given to the adaptability of the proposed framework under extreme climatic conditions and for novel building envelope systems. Second, in the PMV model, fixed values were adopted for parameters such as metabolic rate and clothing insulation, limiting the model's applicability across diverse usage scenarios. Future research could be advanced in three directions. First, the scope of study could be broadened by incorporating additional green materials and datasets from complex climate zones to enhance model generalizability. Second, the coupling of multi-physics fields could be deepened by integrating CFD to capture the dynamic influence of airflow patterns, enabling the development of a multi-dimensional predictive model that considers temperature, humidity, air velocity, and radiation. Third, the adoption of intelligent optimization techniques, such as machine learning, could facilitate the refinement of parametric mapping relationships—enabling a shift from data-driven simulation to intelligent predictive optimization—thereby offering more efficient solutions for the full life-cycle performance enhancement of green buildings.

REFERENCES

[1] Batool, K., Ali, G., Ullah Khan, K., Asif Kamran, M., Yan, N. (2024). Integrating role of green buildings in achieving carbon neutrality in an era of climate emergency. Sustainable Development, 32(4): 4186-4201. https://doi.org/10.1002/sd.2883

[2] Wei, J.Q., Zhou, Z.H., Yu, Q., Xie, J.W., Cheng, X., Hong, Y.X. (2024). Analyzing Technical barriers to green farmhouse construction in China: A DEMATEL-ISM-MICMAC Approach. Journal of Green Economy and Low-Carbon Development, 3(2): 106-121.

https://doi.org/10.56578/jgelcd030204

[3] Lakhiar, M.T., Sanmargaraja, S., Olanrewaju, A., Lim, C.H., Ponniah, V., Mathalamuthu, A.D. (2024). Evaluating and comparing objective and subjective thermal comfort in a malaysian green office building: A case study. Case Studies in Thermal Engineering, 60: 104614. https://doi.org/10.1016/j.csite.2024.104614

[4] Elnaklah, R., Walker, I., Natarajan, S. (2021). Moving to a green building: Indoor environment quality, thermal comfort and health. Building and Environment, 191: 107592. https://doi.org/10.1016/j.buildenv.2021.107592

[5] Kim, J., Hong, T., Jeong, J., Koo, C., Jeong, K. (2016). An optimization model for selecting the optimal green systems by considering the thermal comfort and energy consumption. Applied Energy, 169: 682-695. https://doi.org/10.1016/j.apenergy.2016.02.032

[6] Mousavi, S., Gheibi, M., Wacławek, S., Behzadian, K. (2023). A novel smart framework for optimal design of green roofs in buildings conforming with energy conservation and thermal comfort. Energy and Buildings, 291: 113111. https://doi.org/10.1016/j.enbuild.2023.113111

[7] Olugboyega, O. (2024). Differential relationships in the BIM implementation process in a developing country: The role of essential BIM implementation strategies. Engineering, Construction and Architectural Management, 31(8): 3283-3307. https://doi.org/10.1108/ECAM-10-2022-0999

[8] Smits, W., van Buiten, M., Hartmann, T. (2017). Yield-to-BIM: Impacts of BIM maturity on project performance. Building research & information, 45(3): 336-346. https://doi.org/10.1080/09613218.2016.1190579

[9] Ghanbari, M., Zolfaghari, D., Yadegari, Z. (2023). Mitigating construction delays in Iran: An empirical evaluation of building information modeling and integrated project delivery. Journal of Engineering Management and Systems Engineering, 2(3): 170-179. https://doi.org/10.56578/jemse020304

[10] Polo-Labarrios, M.A., Quezada-García, S., Sánchez-Mora, H., Escobedo-Izquierdo, M.A., Espinosa-Paredes, G. (2020). Comparison of thermal performance between green roofs and conventional roofs. Case Studies in Thermal Engineering, 21: 100697. https://doi.org/10.1016/j.csite.2020.100697

[11] Li, H. X., Ma, Z., Liu, H., Wang, J., Al-Hussein, M., Mills, A. (2020). Exploring and verifying BIM-based energy simulation for building operations. Engineering, Construction and Architectural Management, 27(8): 1679-1702. https://doi.org/10.1108/ECAM-06-2019-0314

[12] Carvalho, J.P., Almeida, M., Bragança, L., Mateus, R. (2021). Bim-based energy analysis and sustainability assessment—Application to Portuguese buildings. Buildings, 11(6): 246. https://doi.org/10.3390/buildings11060246

[13] Calcerano, F., Thravalou, S., Martinelli, L., Alexandrou, K., Artopoulos, G., Gigliarelli, E. (2024). Energy and environmental improvement of built heritage: HBIM simulation-based approach applied to nine Mediterranean case-studies. Building Research & Information, 52(1-2): 225-247. https://doi.org/10.1080/09613218.2023.2204417

[14] Kim, H., Shen, Z., Kim, I., Kim, K., Stumpf, A., Yu, J. (2016). BIM IFC information mapping to building energy analysis (BEA) model with manually extended material information. Automation in Construction, 68: 183-193. https://doi.org/10.1016/j.autcon.2016.04.002

[15] Punnathanam, V., Kotecha, P. (2016). Effective multi-objective optimization of Stirling engine systems. Applied Thermal Engineering, 108: 261-276. https://doi.org/10.1016/j.applthermaleng.2016.07.029

[16] Punnathanam, V., Kotecha, P. (2017). Multi-objective optimization of Stirling engine systems using Front-based Yin-Yang-Pair Optimization. Energy Conversion and Management, 133: 332-348. https://doi.org/10.1016/j.enconman.2016.10.035

[17] Conceição, E., Gomes, J., Awbi, H. (2019). Influence of the airflow in a solar passive building on the indoor air quality and thermal comfort levels. Atmosphere, 10(12): 766. https://doi.org/10.3390/atmos10120766

[18] Gwak, J., Shino, M., Ueda, K., Kamata, M. (2019). An investigation of the effects of changes in the indoor ambient temperature on arousal level, thermal comfort, and physiological indices. Applied Sciences, 9(5): 899. https://doi.org/10.3390/app9050899